Several phase II studies demonstrated antitumor activity of the purine analogs fludarabine and cladribine [37,38]. Chemotherapy alone (such as alkylating agent) series reported the significantly higher recurrence rate and cannot be the standard therapy for local advanced gastric MALT lymphoma [39–41]. Other groups have also shown that the anti-CD20 monoclonal antibody rituximab was effective for MALT lymphoma [42,43]. These findings also will be further elucidated in large-scale clinical trials.

According to Hellenic Cooperative Oncology Group's study [46], their patients received various commonly used chemotherapy regimens. Anthracycline-based treatments or rituximab did not offer any survival advantages. As rituximab therapy was started only recently, the follow-up, however, may have been too short to reveal any benefit. Other retrospective studies also observed no difference in efficacy between specific regimens [44,45], and several prospective phase II trials reported similar results [41,42,47,48].

The most frequent sites in this study were the stomach, the orbital adnexa, the head and neck, and the small bowel. Despite the low number of patients in our study, this observation is in agreement with other studies reporting the salivary glands, the orbit, the lung, the intestine and the skin as the most common nongastric lymphoma sites [13,43–46].

The next problem that should be resolved is the optimal target volume for MALT lymphoma. There are only a few studies that clearly demonstrate the target volume in the literature [16,21–23,25,27–29,31]. For gastric MALT lymphomas, the entire stomach and perigastric nodes are considered to be the target volume [28,29]. Olivier et al. [22] also delivered RT to the affected parotid gland with or without the first-echelon node for parotid lymphoma. On the one hand, Pfeffer et al. [49] showed that 4 of 12 patients with orbital lymphoma who received partial orbital irradiation experienced recurrence. Thus it seems reasonable that the target volume for MALT lymphoma should include the entire affected organ.

Conclusion

In conclusion, the results from this retrospective study confirm that RT was highly effective in achieving local control for localized MALT lymphoma, and 30 Gy in 20 fr was appropriate for controlling MALT lymphoma without severe detrimental effects.

* **Corresponding author. Keiichi Nakagawa**, Department of Radiology, University of Tokyo Hospital, 7-3-1 Hongo, Bunkyo-ku, Tokyo, 113-8655 Japan. *E-mail address:* nakagawa-rad@h.u-tokyo.ac.jp

Received 8 February 2008; received in revised form 14 March 2008; accepted 14 March 2008; Available online 16 April 2008

References

[1] Harris NL, Jaffe ES, Stein H, Banks PM, Chan JK, Cleary ML, et al. A revised European–American classification of lymphoid neoplasms: a proposal from the International Lymphoma Study Group. Blood 1994;84:1361–92.

[2] Harris NL, Jaffe ES, Diebold J, Flandrin G, Muller-Hermelink HK, Vardiman J, et al. World Health Organization classification of neoplastic diseases of the hematopoietic and lymphoid tissues: report of the clinical advisory committee meeting – Airlie House, Virginia, November 1997. J Clin Oncol 1999;17:3835–49.

[3] Armitage JO, Weisenburger DD. New approach to classifying non-Hodgkin's lymphomas: clinical features of the major histologic subtypes. Non-Hodgkin's Lymphoma Classification Project. J Clin Oncol 1998;16:2780–95.

[4] Anderson JR, Armitage JO, Weisenburger DD. Epidemiology of the non-Hodgkin's lymphomas: distributions of the major subtypes differ by geographic locations. Non-Hodgkin's Lymphoma Classification Project. Ann Oncol 1998;9:717–20.

[5] Lymphoma Study Group of Japanese Pathologists: The World Health Organization classification of malignant lymphomas in Japan: incidence of recently recognized entities. Pathol Int 2000;50:696–702.

[6] Bayerdörffer E, Neubauer A, Rudolph B, Thiede C, Lehn N, Eidt S, et al. Regression of primary gastric lymphoma of mucosa-associated lymphoid tissue type after cure of *Helicobacter pylori* infection. MALT Lymphoma Study Group. Lancet 1995;345:1591–4.

[7] Roggero E, Zucca E, Pinotti G, Pascarella A, Capella C, Savio A, et al. Eradication of *Helicobacter pylori* infection in primary low-grade gastric lymphoma of mucosa-associated lymphoid tissue. Ann Intern Med 1995;122:767–9.

[8] Steinbach G, Ford R, Glober G, Sample D, Hagemeister FB, Lynch PM, et al. Antibiotic treatment of gastric lymphoma of mucosa-associated lymphoid tissue. An uncontrolled trial. Ann Intern Med 1999;131:88–95.

[9] Isaacson PG, Diss TC, Wotherspoon AC, Barbazza R, De Boni M, Doglioni C. Long-term follow-up of gastric MALT lymphoma treated by eradication of *H. pylori* with antibodies. Gastroenterology 1999;117:750–1.

[10] Savio A, Zamboni G, Capelli P, Negrini R, Santandrea G, Scarpa A, et al. Relapse of low-grade gastric MALT lymphoma after *Helicobacter pylori* eradication: true relapse or persistence? Long-term post-treatment follow-up of a multicenter trial in the north–east of Italy and evaluation of the diagnostic protocol's adequacy. Recent Results Cancer Res 2000;156:116–24.

[11] Aozasa K. Hashimoto's thyroiditis as a risk factor of thyroid lymphoma. Acta Pathol Jpn 1990;40:459–68.

[12] Tzioufas AG, Boumba DS, Skopouli FN, Moutsopoulos HM. Mixed monoclonal cryoglobulinemia and monoclonal rheumatoid factor cross-reactive idiotypes as predictive factors for the development of lymphoma in primary Sjögren's syndrome. Arthritis Rheum 1996;39:767–72.

[13] Thieblemont C, Bastion Y, Berger F, Rieux C, Salles G, Dumontet C, et al. Mucosa-associated lymphoid tissue gastrointestinal and nongastrointestinal lymphoma behavior: analysis of 108 patients. J Clin Oncol 1997;15:1624–30.

[14] Zucca E, Roggero E, Pileri S. B-cell lymphoma of MALT type: a review with special emphasis on diagnostic and management problems of low-grade gastric tumours. Br J Haematol 1998;100:3–14.

[15] Chao CK, Lin HS, Devineni VR, et al. Radiation therapy for primary orbital lymphoma. Int J Radiat Oncol Biol Phys 1995;31:929–34.

[16] Bolek TW, Moyses HM, Marcus Jr RB, et al. Radiotherapy in the management of orbital lymphoma. Int J Radiat Oncol Biol Phys 1999;44:31–6.

[17] Pelloski CE, Wilder RB, Ha CS, et al. Clinical stage IEA–IIEA orbital lymphomas: outcomes in the era of modern staging and treatment. Radiother Oncol 2001;59:145–51.

[18] Stafford SL, Kozelsky TF, Garrity JA, et al. Orbital lymphoma: radiotherapy outcome and complications. Radiother Oncol 2001;59:139–44.

[19] Le QT, Eulau SM, George TI, et al. Primary radiotherapy for localized orbital MALT lymphoma. Int J Radiat Oncol Biol Phys 2002;52:657–63.
[20] Fung CY, Tarbell NJ, Lucarelli MJ, et al. Ocular adnexal lymphoma: clinical behavior of distinct world health organization classification subtypes. Int J Radiat Oncol Biol Phys 2003;57:1382–91.
[21] Hasegawa M, Kojima M, Shioya M, et al. Treatment results of radiotherapy for malignant lymphoma of the orbit and histopathologic review according to the WHO classification. Int J Radiat Oncol Biol Phys 2003;57:172–6.
[22] Martinet S, Ozsahin M, Belkacemi Y, et al. Outcome and prognostic factor in orbital lymphoma: a rare cancer network study on 90 consecutive patients treated with radiotherapy. Int J Radiat Oncol Biol Phys 2003;55:892–8.
[23] Olivier KR, Brown PD, Stafford SL, et al. Efficacy and treatment-related toxicity of radiotherapy for early-stage primary non-Hodgkin lymphoma of the parotid gland. Int J Radiat Oncol Biol Phys 2004;60:1510–4.
[24] Zhou P, Ng AK, Silver B, et al. Radiation therapy for orbital Lymphoma. Int J Radiat Oncol Biol Phys 2005;3:66–871.
[25] Wenzel C, Fiebiger W, Dieckmann K, et al. Extranodal marginal zone B-cell lymphoma of mucosa-associated lymphoid tissue of the head and neck area. Cancer 2003;67:2236–41.
[26] Tsang RW, Gospodarowicz MK, Pintilie M, et al. Stages I and II MALT lymphoma: results of treatment with radiotherapy. Int J Radiat Oncol Biol Phys 2001;50:1258–64.
[27] Hitchcock S, Ng AK, Fisher DC, et al. Treatment outcome of mucosa-associated lymphoid tissue/marginal zone non-Hodgkin's lymphoma. Int J Radiat Oncol Biol Phys 2002;52:1058–66.
[28] Tsang RW, Gospodarowicz MK, Pintilie M, Wells W, Hodgson DC, Sun A, et al. Localized mucosa-associated lymphoid tissue lymphoma treated with radiation therapy has excellent outcome. J Clin Oncol 2003;21:4157–64.
[29] Schechter NR, Portlock CS, Yahalom J. Treatment of mucosa associated lymphoid tissue lymphoma of the stomach with radiation alone. J Clin Oncol 1998;16:1916–21.
[30] Fung CY, Grossbard ML, Linggood RM, et al. Mucosa-associated lymphoid tissue lymphoma of the stomach. Cancer 1999;85:9–17.
[31] Isobe K, Kagami Y, Higuchi K, Kodaira T, Hasegawa M, Shikama N, et al. Japan Radiation Oncology Group. A multicenter phase II study of local radiation therapy for stage IEA mucosa-associated lymphoid tissue lymphomas: a preliminary report from the Japan Radiation Oncology Group (JAROG). Int J Radiat Oncol Biol Phys 2007;69:1181–6.
[32] Allal A, Kurtz JM, Pipard G, Marti MC, Miralbell R, Popowski Y, et al. Chemoradiotherapy versus radiotherapy alone for anal cancer: a retrospective comparison. Int J Radiat Oncol Biol Phys 1993;27:59–66.
[33] Esik O, Ikeda H, Mukai K, Kaneko A. A retrospective analysis of different modalities for treatment of primary orbital non-Hodgkin's lymphomas. Radiother Oncol 1996;38:13–8.
[34] Sasai K, Yamabe H, Dodo Y, Kashii S, Nagata Y, Hiraoka M. Non-Hodgkin's lymphoma of the ocular adnexa. Acta Oncol 2001;40:485–90.
[35] Lee JL, Kim MK, Lee KH, Hyun MS, Chung HS, Kim DS, et al. Extranodal marginal zone B-cell lymphomas of mucosa-associated lymphoid tissue-type of the orbit and ocular adnexa. Ann Hematol 2005;84:13–8.
[36] Jäger G, Neumeister P, Brezinschek R, Hinterleitner T, Fiebiger W, Penz M, et al. Treatment of extranodal marginal zone B-cell lymphoma of mucosa-associated lymphoid tissue type with cladribine: a phase II study. J Clin Oncol 2002;20:3872–7.
[37] Zinzani PL, Stefoni V, Musuraca G, Tani M, Alinari L, Gabriele A, et al. Fludarabine-containing chemotherapy as frontline treatment of nongastrointestinal mucosa-associated lymphoid tissue lymphoma. Cancer 2004;100:2190–4.
[38] Taal BG, Burgers JM, van Heerde P, Hart AA, Somers R. The clinical spectrum and treatment of primary non-Hodgkin's lymphoma of the stomach. Ann Oncol 1993;4:839–46.
[39] Ruskoné-Fourmestraux A, Aegerter P, Delmer A, Brousse N, Galian A, Rambaud JC. Primary digestive tract lymphoma: a prospective multicentric study of 91 patients. Groupe d'Etude des Lymphomes Digestifs. Gastroenterology 1993;105:1662–71.
[40] Hammel P, Haioun C, Chaumette MT, Gaulard P, Divine M, Reyes F, et al. Efficacy of single-agent chemotherapy in low-grade B-cell mucosa-associated lymphoid tissue lymphoma with prominent gastric expression. J Clin Oncol 1995;13:2524–9.
[41] Conconi A, Martinelli G, Thiéblemont C, Ferreri AJ, Devizzi L, Peccatori F, et al. Clinical activity of rituximab in extranodal marginal zone B-cell lymphoma of MALT type. Blood 2003;102:2741–5.
[42] Martinelli G, Laszlo D, Ferreri AJ, Pruneri G, Ponzoni M, Conconi A, et al. Clinical activity of rituximab in gastric marginal zone non-Hodgkin's lymphoma resistant to or not eligible for anti-*Helicobacter pylori* therapy. J Clin Oncol 2005;23:1979–83.
[43] Zinzani PL, Magagnoli M, Galieni P, Martelli M, Poletti V, Zaja F, et al. Nongastrointestinal low-grade mucosa-associated lymphoid tissue lymphoma: analysis of 75 patients. J Clin Oncol 1999;17:1254–8.
[44] Arcaini L, Burcheri S, Rossi A, Passamonti F, Paulli M, Boveri E, et al. Nongastric marginal-zone B-cell MALT lymphoma: prognostic value of disease dissemination. Oncologist 2006;11:285–91.
[45] Zucca E, Conconi A, Pedrinis E, Cortelazzo S, Motta T, Gospodarowicz MK, et al. International Extranodal Lymphoma Study Group. Nongastric marginal zone B-cell lymphoma of mucosa-associated lymphoid tissue. Blood 2003;101:2489–95.
[46] Papaxoinis G, Fountzilas G, Rontogianni D, Dimopoulos MA, Pavlidis N, Tsatalas C, et al. Low-grade mucosa-associated lymphoid tissue lymphoma: a retrospective analysis of 97 patients by the Hellenic Cooperative Oncology Group (HeCOG). Ann Oncol 2007 Dec 20. Epub ahead of print.
[47] Conconi A, Bertoni F, Pedrinis E, Motta T, Roggero E, Luminari S, et al. Nodal marginal zone B-cell lymphomas may arise from different subsets of marginal zone B lymphocytes. Blood 2001;98:781–6.
[48] Jäger G, Neumeister P, Quehenberger F, Wöhrer S, Linkesch W, Raderer M. Prolonged clinical remission in patients with extranodal marginal zone B-cell lymphoma of the mucosa-associated lymphoid tissue type treated with cladribine: 6 year follow-up of a phase II trial. Ann Oncol 2006;17:1722–3.
[49] Pfeffer MR, Rabin T, Tsvang L, Goffman J, Rosen N, Symon Z. Orbital lymphoma: is it necessary to treat the entire orbit? Int J Radiat Oncol Biol Phys 2004;60:527–30.
[50] Terai S, Iijima K, Kato K, Dairaku N, Suzuki T, Yoshida M, et al. Long-term outcomes of gastric mucosa-associated lymphoid tissue lymphomas after *Helicobacter pylori* eradication therapy. Tohoku J Exp Med 2008;214:79–87.
[51] Suh CO, Shim SJ, Lee SW, Yang WI, Lee SY, Hahn JS. Orbital marginal zone B-cell lymphoma of MALT: radiotherapy results and clinical behavior. Int J Radiat Oncol Biol Phys 2006;65:228–33.
[52] Le QT, Eulau SM, George TI, Hildebrand R, Warnke RA, Donaldson SS, et al. Primary radiotherapy for localized orbital MALT lymphoma. Int J Radiat Oncol Biol Phys 2002;52:657–63.
[53] Zhou P, Ng AK, Silver B, Li S, Hua L, Mauch PM. Radiation therapy for orbital lymphoma. Int J Radiat Oncol Biol Phys 2005;63:866–71.

Case Report

Stereotactic and Functional Neurosurgery

Stereotact Funct Neurosurg 2008;86:231–236
DOI: 10.1159/000131661

Published online: May 13, 2008

Cyst Formation after Stereotactic Radiosurgery for Intracranial Meningioma

Hiroshi Igaki[a] Keisuke Maruyama[b] Masao Tago[a] Masahiro Shin[b]
Naoya Murakami[a] Tomoyuki Koga[b] Keiichi Nakagawa[a] Nobutaka Kawahara[b]
Kuni Ohtomo[a]

Departments of [a]Radiology and [b]Neurosurgery, University of Tokyo Hospital, Tokyo, Japan

Key Words
Meningioma · Cyst formation · Gamma knife radiosurgery

Abstract
The authors report 2 cases of delayed cyst formation after gamma knife radiosurgery for 3 meningioma lesions. All 3 lesions reported here had a distinctive feature before gamma knife treatment of small and spotty intratumoral cysts. One patient experienced an intriguing clinical course of spontaneous regression of the enlarged cyst, and 2 of the 3 lesions became symptomatic requiring surgical interventions. Cyst formation as a postradiosurgical complication is relatively rare in meningioma patients in the literature, and its pathogenesis is unclear. We describe herein the clinical courses of these 2 patients and review the relevant literature in this report. From our experience of these 2 cases, we suggest that we should be aware of the possible development of spotty intratumoral cysts into larger cysts after stereotactic radiosurgery and that we should carefully observe such patients after the treatment.

Introduction

Meningioma is a benign intracranial tumor for which craniotomy and surgical intervention are the standard treatment. Stereotactic radiosurgery has recently been a safe and effective option, especially for high-risk patients for surgery such as those with skull base lesions.

By increasing use of stereotactic radiosurgery for such benign lesions, late radiosurgical complications have well been recognized and focused. Delayed cyst formation is known as one of the complications. It is well known in arteriovenous malformation patients [1–9], and the crude incidence of this symptomatic complication was estimated to be 0.2–0.5% based on a large number of patients [1–3]. Similar complications have been reported for benign tumors such as trigeminal/vestibular schwannomas [10–15], low-grade astrocytomas [16], pituitary adenomas [17, 18] and meningiomas [19–21]. According to these reports, the incidence of delayed cyst formation is estimated to be 0.7–1.7% in meningioma patients after stereotactic radiosurgery, which appears less than that in arteriovenous malformation patients. But reports on this morbidity are scarce, so the true incidence is not known. The pathogenesis of this morbidity remains to be determined.

KARGER
Fax +41 61 306 12 34
E-Mail karger@karger.ch
www.karger.com

1011–6125/08/0864–0231$24.50/0

Accessible online at:
www.karger.com/sfn

Hiroshi Igaki, MD, PhD
Department of Radiology
University of Tokyo Hospital
7-3-1, Hongo, Bunkyo-ku, Tokyo 113-8655 (Japan)
Tel. +81 3 5800 8666, Fax +81 3 5800 8935, E-Mail igaki-tky@umin.ac.jp

Table 1. Summary of the characteristics of tumors with delayed cyst formation

Case No.	Previous surgeries	Tumor location	Subtype	GKR maximal dose and treatment, Gy	GKR margin dose, Gy	Nauta cyst type [27]	Time to cyst development months
1	3	lateral ventricle	meningothelial	36 (first) 36 (fourth)	18 18	II	55
		convexity	atypical	32 (second) 36 (third) 36 (fourth)	16 18 18	II	2
2	2	cavernous sinus	meningothelial	28	14	II	52

The present study reviews and reports the clinical courses of 2 patients with 3 meningioma lesions (table 1) developing delayed cysts after gamma knife radiosurgery (GKR).

Case Report

Case 1

A 46-year-old female patient presented to our hospital with recurrent meningiomas located in the right convexity and in the right lateral ventricle. She had undergone tumor resection 3 times at another hospital. The tumor subtype had been pathologically proven to be meningothelial meningioma at the previous hospital. In December 1998, the recurrent tumor located in the right lateral ventricle was treated by the first GKR with a margin dose of 18 Gy (fig. 1a). Magnetic resonance (MR) images in August 2000 revealed growth of the residual tumor in the right convexity. We performed the second GKR for this tumor in January 2002 (fig. 2a). One month after the second GKR, disturbance of fine movement of the patient's left hand began to be observed. The spotty cyst that had been observed in the convexity on her first visit at our hospital was increased on MR images in April 2002. Subtotal tumor removal with cyst opening under craniotomy was performed in July 2002 (fig. 2b), at which time the pathological diagnosis of atypical meningioma was made. Then, regrowth of the convexity tumor was observed in July 2003. The convexity tumor was accompanied by an increasing cyst in September 2003 (fig. 2c), so the tumor was again removed with the pathological diagnosis of atypical meningioma. We found ischemic necrosis and intratumoral hemorrhage in the surgical specimen, presumably induced by GKR. The tumor consisted of viable dyskaryotic cells with patternless growth and was diagnosed as atypical meningioma (fig. 3). At the second surgery, the frontomedial portion of the tumor was not removed because the tumor was located near the pyramidal tract. Therefore, the third GKR was performed to the convexity residual tumor with a margin dose of 18 Gy postoperatively (fig. 2d), because of the high MIB-1 index of the tumor in the surgical specimen. The lateral ventricle tumor began to regrow in July 2003 with a growing cystic component (fig. 1b). The fourth GKR was carried out for both tumors, because these tumors again regrew in June 2004 (fig. 1c, 2e). After the fourth GKR, both the tumor and the cyst were stable in size, and the patient remained asymptomatic (fig. 1d, 2f). The patient was now under careful observation at the last follow-up of 4 months after the last treatment.

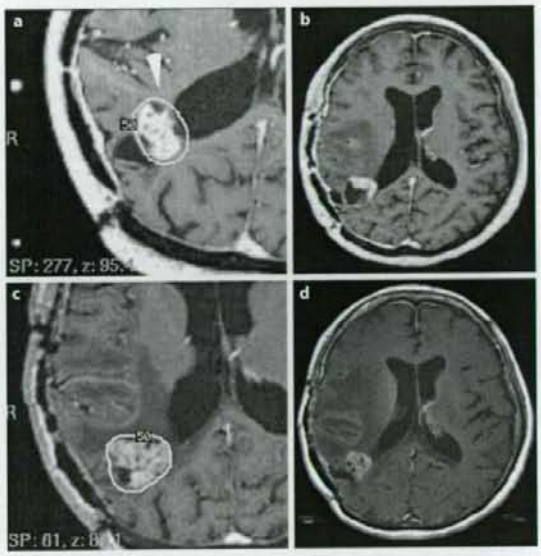

Fig. 1. The tumor of case 1 in the right lateral ventricle. **a** Treatment plan of the first GKR, showing spotty cyst within the tumor as indicated by an arrowhead. **b** An MR image 4.5 years after the first GKR demonstrating tumor regrowth with a cystic component in the posterolateral portion of the tumor. **c** The fourth GKR plan. **d** An MR image 3 months after the fourth GKR with the tumor and the cyst stable in size.

Case 2

A 49-year-old female with meningioma located in the cavernous sinus and clivus consulted (fig. 4a) us presenting with the symptom of double vision. She underwent tumor resection twice

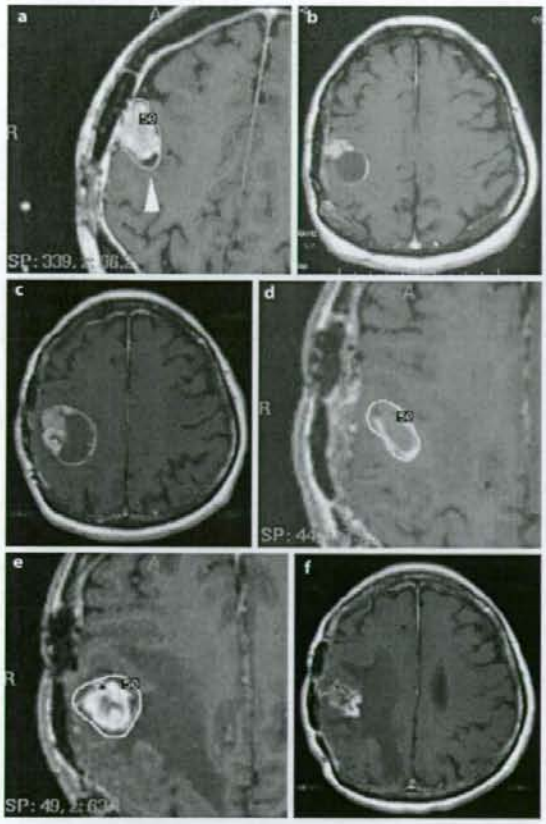

Fig. 2. The tumor of case 1 in the right convexity. **a** Treatment plan of the second GKR (first stereotactic radiosurgery for this convexity lesion). This tumor also had a cystic component within the tumor (arrowhead). **b** An MR image 6 months after the second GKR. The patient developed a symptom of fine movement disturbance of the left hand because of the intratumoral cyst enlargement. She underwent cyst-opening surgery. **c** An MR image 1 year after the surgery showing regrowth of the tumor and the intratumoral cyst. **d** Treatment plan of the third GKR for the residual tumor following the second surgery after **c**. **e** Treatment plan of the fourth GKR for the recurrent tumor. **f** An MR image 3 months after the fourth GKR revealing tumor shrinkage and diminished enhancement of the tumor.

in January and June 1998. The pathological subtype of the tumor was determined as meningothelial meningioma from the surgical specimens. There were no intratumoral cysts at the time of the surgeries. The residual tumor was irradiated by GKR in September 1998 as a planned adjuvant treatment after the second surgery (fig. 4b). At the time of GKR, a cystic component appeared within

Fig. 3. Photomicrograph of the tumor in case 1 presenting ischemic necrosis and intratumoral hemorrhage. HE. Original magnification ×200.

the residual tumor. The cyst began growing 4 years after GKR. Cyst opening was planned in July 2003 because the left foramen of Monro was almost obstructed and the left lateral ventricle was enlarged (fig. 4c). After the patient had been admitted for a planned surgery, spontaneous regression of the cyst was observed, presumably because of the rupture to the third ventricle (fig. 4d). The surgery was therefore canceled, and follow-up examinations were continued. In May 2006, the cyst had again increased in size (fig. 4e) with a symptom of affected visual acuity. The patient then underwent insertion of an Ommaya reservoir into the cyst. At the time of this surgery, no attempt was made for a pathological diagnosis of the cyst wall because of the possibility of damaging surrounding structures. After the surgery, the cyst shrank (fig. 4f), and the symptoms were relieved.

Discussion

In general, cystic meningiomas account for 2–7% of all intracranial meningiomas [22–24]. But there have been few reports of the uncommon late radiation morbidity of cyst formation after stereotactic radiosurgery for meningioma [19–21]. The rate of this morbidity has been estimated to be 0.7–1.7% in these previous reports.

The mechanism of cyst formation is not fully understood. Enlargement of a previous hematoma cavity and radiation-induced necrosis accompanied by breakdown of the blood-brain barrier were proposed to explain cyst formation in arteriovenous malformation [5, 19, 25, 26]. As for meningioma, Shuto et al. [20] have reported 5 me-

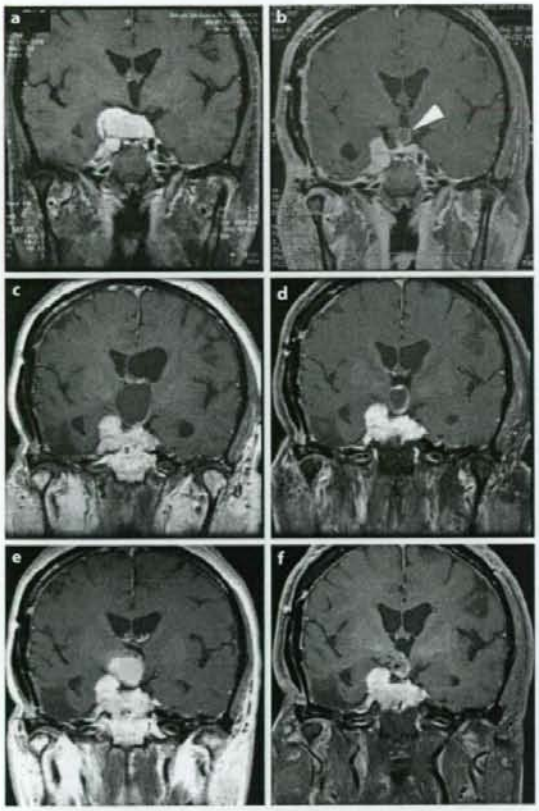

Fig. 4. The tumor of case 2. **a** An MR image of the tumor at the first presentation. Subsequently, the patient underwent 2-staged surgery for tumor removal. **b** An MR image 2 months after the second surgery, revealing a cystic component which had not been observed before, at the periphery of the residual tumor (arrowhead). GKR was performed for this residual tumor as a planned adjuvant treatment after the second surgery. **c** An MR image 4 years after GKR. The cyst was enlarged and almost obstructed the left foramen of Monro. **d** An MR image 10 days after **c**, showing spontaneous regression of the cyst and a relief of the enlarged left lateral ventricle. **e** An MR image 3 years after **d**. The cyst again increased in size with intracystic hemorrhage. **f** An MR image after insertion of an Ommaya reservoir into the cyst. The cyst regressed, and the patient's visual acuity recovered.

ningioma patients developing intratumoral or peritumoral cysts after GKR among 160 treated patients with 184 tumors who were followed up for more than 2 years. They estimated the rate of development of new cysts as 1.7%. They also presumed that delayed cyst formation after stereotactic radiosurgery is caused by ischemic necrosis, increased vascular permeability and intratumoral hemorrhage, based on the pathological findings of their patients' surgical specimens [20]. In addition, the relationship between cyst development and maximal treatment dose in arteriovenous malformation was pointed out [6]. Cyst formation was correlated with radiation-induced brain tissue changes in arteriovenous malformation, although their results did not support a correlation between cyst formation and treatment dose [8]. The treatment dose of 18 Gy at the tumor margin in case 1 was selected to ensure a favorable tumor control, but a higher dose could potentially result in stronger radiation-induced histopathological changes. Considering the results by arteriovenous malformation, a higher dose selection might have promoted a delayed cyst formation in our patients.

In case 1, the pathological subtype was atypical meningioma, with findings of ischemic necrosis and intratumoral hemorrhage, as Shuto et al. [20] pointed out. In case 2, a pathological diagnosis of meningothelial meningioma was made before GKR. Accordingly, it was possible that the cyst was associated with a nonmeningioma lesion such as a Rathke's cleft cyst or craniopharyngioma. This patient had an intriguing and uncommon clinical course where the cyst regressed spontaneously during a period of careful observation during preparations for surgery.

Small spotty cysts were observed at the time of GKR in all 3 tumors that we encountered with developing delayed cysts. Shuto et al. [20] have also reported 2 cases with small intratumoral or peritumoral cystic components (Nauta type II and III [27], respectively) present at the time of GKR that increased in size after treatment. In our patients experiencing delayed cyst formation as well as those of Shuto et al., the incidence of having a cystic component within the pre-GKR tumor was exceptionally high, while a majority of meningiomas do not have intratumoral or peritumoral cysts [22–24]. There might be a risk of delayed cyst formation, and this should be followed up carefully after stereotactic radiosurgery, especially in patients with a cystic component within the meningioma, even if it is small and spotty. Therefore, we recommend obtaining sufficient informed consent of such patients before GKR by revealing the potential risks of morbidities including delayed cyst development.

The pathological subtype of the tumor located in the convexity in case 1 was atypical meningioma (fig. 3), which was in disagreement with the meningothelial subtype diagnosed at the previous hospital. The incidence of tumor recurrence accompanied by dedifferentiation is

reported to be 0.9–2% after surgery and 0.3–2% after stereotactic radiosurgery [19, 28–31]. Histological progression is relatively rare at the recurrence of meningioma. Dedifferentiation may be induced by irradiation or surgery, but the histological grade of recurrent meningioma could sometimes be lower than that of the original tumor [32]. The sampling issues or inter- or intraobserver variability in histological grading might also contribute to changes in tumor grade at recurrence [33]. In our case 1, it is difficult to determine the reason for the change in the histological grade, but the tumor might have undergone treatment-related dedifferentiation change due to GKR or repeated surgeries.

Conclusions

In this report, we have presented 3 lesions in 2 patients of delayed cyst formation after GKR for meningioma. The existence of the pretreatment intratumoral spotty cysts appeared to be related to the cyst enlargement. We should therefore be aware of the possible development of spotty cysts into larger cysts, and carefully observe such patients after stereotactic radiosurgery.

References

1 Flickinger JC, Kondziolka D, Lunsford LD, Pollock BE, Yamamoto M, Gorman DA, Schomberg PJ, Sneed P, Larson D, Smith V, McDermott MW, Miyawaki L, Chilton J, Morantz RA, Young B, Jokura H, Liscak R: A multi-institutional analysis of complication outcomes after arteriovenous malformation radiosurgery. Int J Radiat Oncol Biol Phys 1999;44:67–74.

2 Pollock BE, Brown RD Jr: Management of cysts arising after radiosurgery to treat intracranial arteriovenous malformations. Neurosurgery 2001;49:259–264.

3 Yamamoto M, Ide M, Jimbo M, Hamazaki M, Ban S: Late cyst convolution after gamma knife radiosurgery for cerebral arteriovenous malformations. Stereotact Funct Neurosurg 1998;70(suppl 1):166–178.

4 Edmister WB, Lane JI, Gilbertson JR, Brown RD, Pollock BE: Tumefactive cysts: a delayed complication following radiosurgery for cerebral arterial venous malformations. AJNR Am J Neuroradiol 2005;26:1152–1157.

5 Hara M, Nakamura M, Shiokawa Y, Sawa H, Sato E, Koyasu H, Saito I: Delayed cyst formation after radiosurgery for cerebral arteriovenous malformation: two case reports. Minim Invasive Neurosurg 1998;41:40–45.

6 Izawa M, Hayashi M, Chernov M, Nakaya K, Ochiai T, Murata N, Takasu Y, Kubo O, Hori T, Takakura K: Long-term complications after gamma knife surgery for arteriovenous malformations. J Neurosurg 2005;102 (suppl):34–37.

7 Kim MS, Lee SI, Sim JH: A case of very large cyst formation with gamma knife radiosurgery for an arteriovenous malformation. Stereotact Funct Neurosurg 1999;72(suppl 1):168–174.

8 Pan HC, Sheehan J, Stroila M, Steiner M, Steiner L: Late cyst formation following gamma knife surgery of arteriovenous malformations. J Neurosurg 2005;102(suppl): 124–127.

9 Yamamoto M, Hara M, Ide M, Ono Y, Jimbo M, Saito I: Radiation-related adverse effects observed on neuro-imaging several years after radiosurgery for cerebral arteriovenous malformations. Surg Neurol 1998;49:385–397.

10 Akiyama T, Ikeda E, Kawase T, Yoshida K: Pseudocapsule formation after gamma knife radiosurgery for trigeminal neurinoma – case report. Neurol Med Chir (Tokyo) 2005; 45:526–529.

11 Chung WY, Liu KD, Shiau CY, Wu HM, Wang LW, Guo WY, Ho DM, Pan DH: Gamma knife surgery for vestibular schwannoma: 10-year experience of 195 cases. J Neurosurg 2005;102(suppl):87–96.

12 Hasegawa T, Kida Y, Yoshimoto M, Koike J, Goto K: Evaluation of tumor expansion after stereotactic radiosurgery in patients harboring vestibular schwannomas. Neurosurgery 2006;58:1119–1128.

13 Kwon Y, Khang SK, Kim CJ, Lee DJ, Lee JK, Kwun BD: Radiologic and histopathologic changes after gamma knife radiosurgery for acoustic schwannoma. Stereotact Funct Neurosurg 1999;72(suppl 1):2–10.

14 Landy HJ, Markoe AM, Wu X, Patchen SJ, Reis IM, Takita C, Abdel-Wahab MM, Wen BC, Wolfson AH, Huang DT: Safety and efficacy of tiered limited-dose gamma knife stereotactic radiosurgery for unilateral acoustic neuroma. Stereotact Funct Neurosurg 2004;82:147–152.

15 Pan L, Wang EM, Zhang N, Zhou LF, Wang BJ, Dong YF, Dai JZ, Cai PW: Long-term results of Leksell gamma knife surgery for trigeminal schwannomas. J Neurosurg 2005; 102(suppl):220–224.

16 Kida Y, Kobayashi T, Mori Y: Gamma knife radiosurgery for low-grade astrocytomas: results of long-term follow-up. J Neurosurg 2000;93(suppl 3):42–46.

17 Iwai Y, Yamanaka K, Yoshioka K: Radiosurgery for nonfunctioning pituitary adenomas. Neurosurgery 2005;56:699–705.

18 Tung GA, Noren G, Rogg JM, Jackson IM: MR imaging of pituitary adenomas after gamma knife stereotactic radiosurgery. AJR Am J Roentgenol 2001;177:919–924.

19 Pollock BE: Stereotactic radiosurgery for intracranial meningiomas: indications and results. Neurosurg Focus 2003;14:E4.

20 Shuto T, Inomori S, Fujino H, Nagano H, Hasegawa N, Kakuta Y: Cyst formation following gamma knife surgery for intracranial meningioma. J Neurosurg 2005;102(suppl): 134–139.

21 Stafford SL, Pollock BE, Foote RL, Link MJ, Gorman DA, Schomberg PJ, Leavitt JA: Meningioma radiosurgery: tumor control, outcomes, and complications among 190 consecutive patients. Neurosurgery 2001;49: 1029–1037, discussion 1037–1028.

22 Fortuna A, Ferrante L, Acqui M, Guglielmi G, Mastronardi L: Cystic meningiomas. Acta Neurochir (Wien) 1988;90:23–30.

23 Jung TY, Jung S, Shin SR, Moon KS, Kim IY, Park SJ, Kang SS, Kim SH: Clinical and histopathological analysis of cystic meningiomas. J Clin Neurosci 2005;12:651–655.

24 Sridhar K, Ravi R, Ramamurthi B, Vasudevan MC: Cystic meningiomas. Surg Neurol 1995;43:235–239.

25 Kihlström L, Guo WY, Karlsson B, Lindquist C, Lindqvist M: Magnetic resonance imaging of obliterated arteriovenous malformations up to 23 years after radiosurgery. J Neurosurg 1997;86:589–593.

▶26 Yamamoto M, Jimbo M, Hara M, Saito I, Mori K: Gamma knife radiosurgery for arteriovenous malformations: long-term follow-up results focusing on complications occurring more than 5 years after irradiation. Neurosurgery 1996;38:906–914.
▶27 Nauta HJ, Tucker WS, Horsey WJ, Bilbao JM, Gonsalves C: Xanthochromic cysts associated with meningioma. J Neurol Neurosurg Psychiatry 1979;42:529–535.
▶28 Rohringer M, Sutherland GR, Louw DF, Sima AA: Incidence and clinicopathological features of meningioma. J Neurosurg 1989; 71:665–672.
▶29 Jääskeläinen J, Haltia M, Laasonen E, Wahlström T, Valtonen S: The growth rate of intracranial meningiomas and its relation to histology. An analysis of 43 patients. Surg Neurol 1985;24:165–172.
▶30 Malik I, Rowe JG, Walton L, Radatz MW, Kemeny AA: The use of stereotactic radiosurgery in the management of meningiomas. Br J Neurosurg 2005;19:13–20.
▶31 Noël G, Bollet MA, Calugaru V, Feuvret L, Haie-Meder C, Dhermain F, Ferrand R, Boisserie G, Beaudré A, Mazeron JJ, Habrand JL: Functional outcome of patients with benign meningioma treated by 3D conformal irradiation with a combination of photons and protons. Int J Radiat Oncol Biol Phys 2005;62:1412–1422.
▶32 Perry A, Stafford SL, Scheithauer BW, Suman VJ, Lohse CM: Meningioma grading: an analysis of histologic parameters. Am J Surg Pathol 1997;21:1455–1465.
▶33 Commins DL, Atkinson RD, Burnett ME: Review of meningioma histopathology. Neurosurg Focus 2007;23:E3.

Jpn J Clin Oncol 2008;38(6)438–444
doi:10.1093/jjco/hyn038

Three-dimensional Conformal Radiotherapy for Hepatocellular Carcinoma with Inferior Vena Cava Invasion

Hiroshi Igaki[1], Keiichi Nakagawa[1], Kenshiro Shiraishi[1], Shuichiro Shiina[2], Norihiro Kokudo[3], Atsuro Terahara[1], Hideomi Yamashita[1], Nakashi Sasano[1], Masao Omata[2] and Kuni Ohtomo[1]

[1]Departments of Radiology, [2]Gastroenterology and [3]Hepato-Biliary-Pancreatic Surgery, The University of Tokyo Hospital, Tokyo, Japan

Received February 25, 2008; accepted April 24, 2008; published online May 21, 2008

Background: Hepatocellular carcinoma with inferior vena cava invasion is a rare but fatal condition of disease progression. The aim of this study was to analyze the results of treatment for hepatocellular carcinoma with inferior vena cava invasion by three-dimensional conformal radiation therapy.
Methods: From 1990 to 2006, 18 histopathologically confirmed hepatocellular carcinoma patients with inferior vena cava invasion who were unsuitable for surgery were treated by three-dimensional conformal radiation therapy at our hospital with two to four static or dynamic conformal arc fields.
Results: A median total tumor dose of 50 Gy (range 30–60 Gy) was delivered. The progression-free rate was 91.6% among the patients in whom follow-up computed tomography was obtained. Actuarial survival at 1 year was 33.3%, and the median survival period was 5.6 months.
Conclusions: Three-dimensional conformal radiation therapy might offer a chance of long survival for a part of the hepatocellular carcinoma patients with inferior vena cava invasion, since a third of such patients survived more than a year. Additional treatments should be considered to prevent distant metastases and hepatic functional deterioration after three-dimensional conformal radiation therapy.

Key words: hepatocellular carcinoma – inferior vena cava – three-dimensional conformal radiation therapy – hepatic functional reserve – liver cirrhosis

INTRODUCTION

Hepatocellular carcinoma (HCC) is the eighth major cause of cancer death in the United States and the third in Japan (1,2). Local ablative therapies such as hepatectomy, radiofrequency ablation (RFA) and percutaneous ethanol injection (PEI) should be administered, if possible, to patients with limited extension of HCC. But when the tumor invades the inferior vena cava (IVC), these treatments are indicated only for very few patients. In some reports, a part of these patients can survive long by hepatic resection combined with IVC resection (3–5). But such aggressive surgeries are not suitable for most patients, and other treatment modalities are also restricted not only by poor hepatic function, but also frequently by extensive disease progression. Transcatheter arterial chemoembolization (TACE) is often tried in HCC patients with IVC invasion for whom ablative treatment is unsuitable. However, TACE rarely achieves local tumor control to prolong survival periods sufficiently in such a critical condition, although the efficacy of this treatment has been proven in meta-analyses (6,7).

A few decades ago, liver was assumed to be a highly radiosensitive organ that was unsuitable for high-dose radiotherapy. But recent progress in radiation oncology has enabled us to concentrate high-dose radiation on liver tumors while preserving hepatic function after treatment (8–15). In addition, some institutions apply stereotactic radiotherapy to solitary small liver tumors. Consequently, radiotherapy has come to play an important role in multidisciplinary treatment of HCC.

At our institution, three-dimensional conformal radiation therapy (3D-CRT) has been the primary treatment strategy for HCC with portal vein invasion, and has achieved good clinical results (9). As with the treatment of HCC patients

For reprints and all correspondence: Hiroshi Igaki, Department of Radiology, The University of Tokyo Hospital, 7-3-1, Hongo, Bunkyo-ku, Tokyo 113-8655, Japan. E-mail: igaki-tky@umin.ac.jp

with portal vein invasion, radiotherapy is considered for HCC patients with IVC invasion at our institution if they are unsuitable for surgery. But there are few reports on radiotherapy for such patients (16), and the natural course of such conditions is not well known. In the present study, we retrospectively reviewed the medical records of HCC patients with IVC invasion and analyzed the efficacy of radiotherapy in these patients.

METHODS

From 1990 to 2006, 18 HCC patients with IVC invasion were treated by radiotherapy at our hospital. Their clinical courses and treatment results were retrospectively reviewed. HCC was diagnosed by using ultrasonography, computed tomography (CT), angiography and liver biopsy. In each patient, the diagnosis was confirmed histopathologically. IVC invasion was defined by a low-attenuation mass that protruded into the intraluminal space of IVC on enhanced CT and/or detection of pulsatile flow in IVC thrombi by Doppler ultrasonography. The patients' characteristics are shown in Table 1.

Patients with liver cirrhosis of Child–Pugh class C were not indicated for the treatment. CT-based radiotherapy treatment planning was made for all patients by the following treatment planning systems, RPS700U(3D) (Mitsubishi Electric Co., Tokyo, Japan) or Pinnacle[3] (Philips/ADAC, Milpitas, CA, USA). Clinical target volume was contoured on serial CT images with a 0.5–1-cm margin around the gross tumor volume, covering IVC-protruding tumor as well as the primary tumor invading to the IVC. Other co-existing intrahepatic tumors which had no continuity to the IVC-invading tumor were not included in the clinical target volume, and managed by other treatment modalities. Planning target volume was determined by a 0.5–2.0-cm margin around the clinical target volume. A dynamic conformal arc or two to four static ports were used for irradiation. In earlier periods, dynamic conformal arc therapy or multiport (mainly four ports) treatment plans were used, and we could not obtain dose-volume histograms in the treatment-planning machine. In recent years, treatment plans using two opposed fields have been preferred, because such treatment enables the maximization of the non-irradiated volume of the normal liver tissue. This treatment planning strategy is based on the fact that the normal liver tissue tolerance is lower in patients with viral hepatitis and liver cirrhosis than

Table 1. Patient characteristics

Case no.	Age and sex	Previous treatment				Etiology	Child–Pugh class	Pre-treatment AFP (ng/mL)[1]	Pre-treatment PIVKAII (mAu/mL)[2]
		Surgery	TACE	PEI	RFA				
1	48M	Information not available				HBV	A	38	1
2	67M	Information not available				HBV	B	60	8
3	63M	○		○		Unknown	A	9	N/A
4	67M			○		HCV	A	2385	125
5	80F	Information not available				HCV	A	3	1134
6	58M		○			Alcohol	B	9	26622
7	45M	○	○			HBV	B	136260	10784
8	71M		○		○	HCV	B	4	3242
9	74M		○			HCV	B	10	88
10	70M		○			HCV	B	13	7207
11	61M		○			HCV	B	21	3639
12	72M	○	○	○	○	HCV	A	6175	28
13	70M		○			HCV	B	126	39
14	76M		○			HCV	B	20	3572
15	71M	○	○			HCV	A	11	538
16	74M		○	○	○	HCV	A	38	681
17	69F		○		○	HCV	B	8	1119
18	81M	○	○	○	○	HCV	A	1	12008

Open circles indicate that the patient has received the specific treatment(s). M, male; F, female; TACE, transcatheter arterial chemoembolization; PEI, percutaneous ethanol injection; RFA, radiofrequency ablation; HBV, hepatitis B virus; HCV, hepatitis C virus; N/A, not available; PIVKAII, protein induced by Vitamin K absence-II.

[1]Normal range of serum concentration of AFP is <9 ng/mL.

[2]Normal range of serum concentration of PIVKAII is <40 mAu/mL.

in healthy patients (8). The general principle of treatment planning was to keep V_{30}, which was defined as the percent volume of the liver exceeding 30 Gy, lower than 30% of the whole liver volume minus tumor volume. We aimed for a total tumor dose of 50–60 Gy in conventional fractionation, but allowed smaller doses according to the dose-volume histogram of the normal liver at the physician's discretion. X-rays were delivered by linear accelerators ML15-MDX (Mitsubishi Electric Co., Tokyo, Japan) or CRS-6000 (Mitsubishi Electric Co., Tokyo, Japan). Written informed consent was obtained from the patients before treatment.

Follow-up and survival periods were calculated from the first day of radiation therapy. Actuarial survival rates were calculated by the Kaplan–Meier method. The statistical significance between groups was assessed with the log-rank test. Differences were considered statistically significant when $P < 0.05$.

RESULTS

All patients tolerated the treatment well. No severe complications were observed during the treatment period. The total tumor dose ranged from 30 to 60 Gy, with a median dose of 50 Gy (Table 2). All patients were followed until death except for the three patients who were alive at the time of analysis. Other treatment variables and results are summarized in Table 2.

Treatment response was defined as the tumor status at the last follow-up CT (Table 2). The response rate (complete response + partial response) and progression-free rate (complete response + partial response + stable disease) were 33.3% (95% confidential interval: 6.7–60.0%) and 91.6% (95% confidential interval: 75.9–100%), respectively, among the 12 patients for whom follow-up CTs were obtained. Only one patient developed local progression of the IVC-invading tumor within 6 months after 3D-CRT, and this was determined to be a progressive disease. This patient started systemic chemotherapy with 5-fluorouracil and interferon after diagnosis of a progressive disease, and was alive at the time of this analysis with no further progression of the tumor after introduction of this chemotherapy, 26.2 months after treatment. In the remaining 11 patients, no tumor regrowth was observed within the irradiated volume at the last follow-up.

At the time of the last follow-up, three patients were alive and the others were dead. Actuarial survival rate was 33.3% at 1 year, with a median survival period of 5.6 months (Fig. 1). The causes of death are shown in Table 2. The Child–Pugh class A group tended to survive longer than the class B group, but the difference did not reach statistical significance level (7.8 months versus 3.3 months, $P = 0.136$, Fig. 2 and Table 3). The survival period did not differ between responders (complete response + partial response) and non-responders (stable disease + progressive disease) (Fig. 3 and Table 3). Older patients (70 years or older) and

Table 2. Treatment-related variables and results

Case no.	Total dose (Gy)	Equivalent dose (Gy)[1]	Irradiation technique	Treatment response	Follow-up period (months)	Cause of death
1	48	52	Opposed two fields	N/A	5.6	Unknown
2	48	52	Dynamic conformal	N/A	3.0	Unknown
3	30	37.5	Dynamic conformal	N/A	7.2	Unknown
4	42	42	Dynamic conformal	N/A	1.3	Pulmonary metastasis
5	60	60	Dynamic conformal	CR	7.8	Non-tumoral Liver failure
6	50	50	Dynamic conformal	N/A	3.7	Rupture of esophageal varix
7	50	50	Four fields	SD	3.3	Tumor-related Liver failure
8	46	46	Four fields	SD	2.6	Non-tumoral Liver failure
9	50	50	Four fields	PR	7.2	Pulmonary metastasis
10	50	50	Dynamic conformal	PR	16.3	Non-tumoral Liver failure
11	40	40	Four fields	SD	1.8	Pulmonary metastasis
12	50	50	Dynamic conformal	CR	13.7	Tumor-related Liver failure
13	52	52	Four fields	N/A	1.6	Pulmonary embolization
14	46	46	Opposed two fields	SD	4.7	Tumor-related Liver failure
15	50	50	Four fields	SD	14.5	Brain metastasis
16	50	50	Non-coplanar	PD	26.2	(Alive)
17	40	40	Opposed two fields	SD	12.6	(Alive)
18	50	50	Opposed two fields	SD	10.2	(Alive)

CR, complete response; PR, partial response; SD, stable disease; PD, progressive disease.
[1]Equivalent dose in conventional fractionation of 2.0 Gy per fraction was calculated based on a linear quadratic model assuming $\alpha/\beta = 10$ (32).

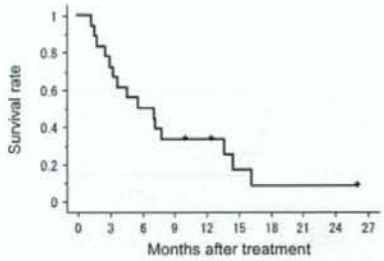

Figure 1. Overall survival of the whole group of 18 patients.

patients with hepatitis C virus tended to survive longer than the other patients, but the differences were also not statistically significant (Fig. 4). The median survival periods were 7.8 and 3.3 months for the groups 70 years or older and under 70 years, respectively ($P = 0.064$). The median survival periods of the patients with HCV carriers and other etiologies were 7.8 and 3.7 months, respectively ($P = 0.111$). A representative case is shown in Fig. 5.

Table 3. Univariate analysis of potential prognostic factors

Factor	*n*	Median survival (months)	*P* value
Etiology			
HCV	13	7.8	0.111
Others	5	3.7	
Treatment response			
Responders	4	7.8	0.894
Non-responders	8	4.6	
Age at treatment			
≥ 70	10	7.8	0.064
< 70	8	3.3	
Child–Pugh class			
A	8	7.8	0.136
B	10	3.3	
Pre-treatment AFP			
≤ 20 ng/mL	10	7.2	0.305
> 20 ng/mL	8	3.0	
Pre-treatment PIVKA II			
≤ 1000 mAu/mL	9	5.6	0.987
> 1000 mAu/mL	9	4.7	

DISCUSSION

HCC with IVC invasion is difficult to treat and associated with poor prognosis, because of its inherent nature of serious condition of the disease and the limited availability of treatment strategies. We have treated such patients by 3D-CRT, and here reviewed their treatment results retrospectively.

The literature offers no detailed data on the natural history of HCC with IVC invasion. But vascular invasion from HCC has been associated with miserable prognoses (16–18) and a limited life expectancy of 2–3 months, if untreated. However, Mizumoto et al. (19) reported good clinical results of proton beam therapy in patients with HCC invading to the IVC. All three of the patients they treated lived more than a year after this therapy.

The prognosis of patients with HCC is known to be dependent on the hepatic functional reserve (20,21). Our results are consistent with this knowledge, because the median survival of Child–Pugh class A patients was slightly longer than that of class B patients (Fig. 2). On the other hand, treatment response did not influence patients' survival periods (Fig. 3). But the treatment response after radiotherapy is predictive of survival in the curative treatment settings in many primary cancer sites (22–24). There are three possible explanations for this: (i) a relatively long period (typically several months) is required for tumor shrinkage after radiotherapy, considering the median survival periods of these patients; (ii) fatal deterioration of hepatic function can be seen, owing to the damage to normal liver tissue as a result of radiotherapy; (iii) it is sometimes difficult to distinguish the tumor thrombus from blood clots adhering to the IVC-invading tumor on follow-up CT images; and (iv) the group in this analysis was too small for statistical differences. Older age was a marginally significant prognostic factor in our results (Fig. 4). Age as a prognostic factor,

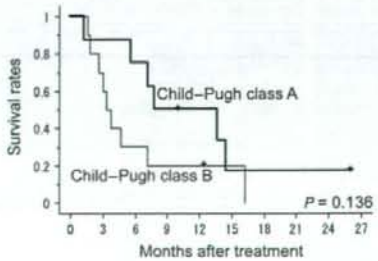

Figure 2. Overall survival by pre-treatment hepatic functional reserve.

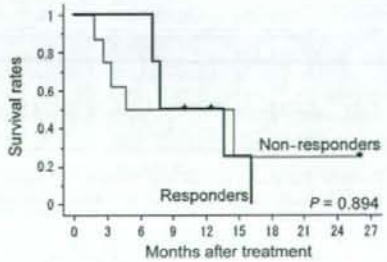

Figure 3. Overall survival by treatment response.

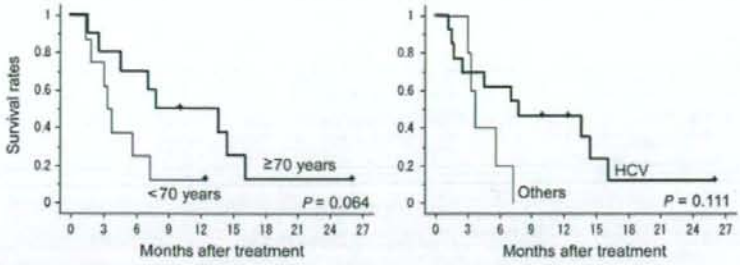

Figure 4. Overall survival by age (left panel) or etiology (right panel).

however, is controversial in the literature, because older age might sometimes be a favorable prognostic factor in some conditions but an unfavorable one in others (25–27).

In our experience, six patients died of liver failure. Of these six, three were assumed to be owing to the intrahepatic tumor growth from their clinical courses, and the other three were brought by undetermined causes. We could not differentiate the natural course of cirrhosis from treatment-related liver failure exactly. In this respect, we could not exclude the possibility of the treatment-related morbidities in Cases 5, 8 and 10 in Tables 1 and 2 with liver failures, although there had been no case with clinically apparent radiation-induced liver disease (RILD). In addition, there is no denying that the rupture of esophageal varix and the pulmonary embolization have occurred irrelevant to 3D-CRT or other treatments in Cases 6 and 13. But after 3D-CRT, 33.3% of our patients survived more than a year. In this respect, our 3D-CRT appeared to offer a chance to survive more than a year for a third of the patients with such critical conditions, although the median survival period was not satisfactory. The reason for such unsatisfactory results included the high incidence of deaths due to metastatic disease or liver failure despite the good progression-free rate of 91.6% for the irradiated IVC-invading tumor.

To minimize the probability of radiotherapy-related liver failure, treatment strategies have been improved (28,29). Despite these efforts, RILD can sometimes occur typically 2 weeks to 4 months after hepatic irradiation, and the threshold for RILD is reported to be 31 Gy of mean liver dose (29). Moreover, 50–76% of the patients who developed RILD died of this complication (30,31). Considering these situations, 3D-CRT has a potential benefit over the conventional two-dimensional radiotherapy in the viewpoint of normal liver protection. This point, however, has not been demonstrated in the previous literature to the best of our knowledge.

Some institutions adopt stereotactic body radiotherapy by multi-port irradiation technique. But the volume of low-dose-irradiated normal liver tissue is increased by the multi-port irradiation, especially when the clinical target volume is large. Radiation tolerance of the non-cancerous liver with chronic viral hepatitis or cirrhosis is known to be lower than that of healthy liver (29). We have a hypothesis that two opposed fields radiotherapy might be more protective than multiple-port radiotherapy for the cirrhotic liver. This is why we changed the 3D-CRT strategy from multiple-port irradiation to two opposed fields irradiation. We are now under investigation of the effect of treatment strategy on the survival or on the risk of RILD.

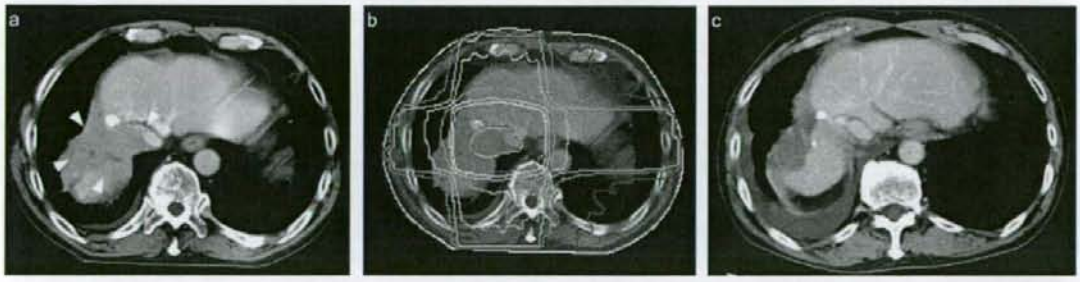

Figure 5. A representative case of a 72-year-old male with Child–Pugh class A hepatic function (case 12 in the Tables 1 and 2). (a) Before radiotherapy, the tumor located in S7 extended to IVC and the intraluminal space was narrow in the CT images. The tumor was indicated by the red arrowhead. (b) Dose distribution of the treatment plan. A total tumor dose of 50 Gy was delivered in 25 fractions by a dynamic conformal arc with four static fields. (c) Three months after radiotherapy. S7 tumor disappeared and no enhancement defect was observed within IVC, and the treatment response was judged as a complete response. The patient died of hepatic failure 13.7 months after irradiation. The irradiated tumor had no sign of regrowth at the time of death. (A colour version of this figure is available as supplementary data at http://www.jjco.oxfordjournals.org.)

Follow-up CT could not be obtained for six patients. This might be attributable in part to early deterioration in performance status, since all six died within 8 months after treatment. It is possible that disease control was not achieved in these patients and that the progression-free rate of 91.6% was thus overestimated. In this respect, additional treatments should be considered as many patients developed distant metastases or hepatic functional deterioration shortly after 3D-CRT.

CONCLUSIONS

A part of the HCC patients with IVC invasion might have benefited from 3D-CRT and a third of such patients had had a chance of surviving more than a year; otherwise they could not have survived long with this progressive fatal disease. However, further treatment should be considered to prevent distant metastasis and to protect post-treatment hepatic function, because the majority of the patients died from metastatic diseases or liver failure in spite of good local tumor control by 3D-CRT.

Funding

This work was supported by grants-in-aid for scientific research from the Ministry of Education, Science, and Culture of Japan (18790877 to H.I.).

Conflict of interest statement

None declared.

References

1. Surveillance Epidemiology and End Results NCI, US National Institute of Health [homepage on the Internet]. Summary of changes in cancer mortality, 1950–2004 and 5-year relative survival rates, 1950–2003 [cited 2008 February 26]. Available format: http://seer.cancer.gov/csr/1975_2004/results_single/sect_01_table.03.pdf.
2. Center for Cancer Control and Information Services, National Cancer Center, Japan [homepage on the Internet]. Graph database, Cancer information service for medical staff [cited 2008 February 26]. Available at: http://ganjoho.ncc.go.jp/pro/statistics/en/graph_db_index.html.
3. Arii S, Teramoto K, Kawamura T, Takamatsu S, Sato E, Nakamura N, et al. Significance of hepatic resection combined with inferior vena cava resection and its reconstruction with expanded polytetrafluoroethylene for treatment of liver tumors. *J Am Coll Surg* 2003;196:243–9.
4. Sarmiento JM, Bower TC, Cherry KJ, Farnell MB, Nagorney DM. Is combined partial hepatectomy with segmental resection of inferior vena cava justified for malignancy? *Arch Surg* 2003;138:624–30; discussion 630–1.
5. Hemming AW, Reed AI, Langham MR, Jr, Fujita S, Howard RJ. Combined resection of the liver and inferior vena cava for hepatic malignancy. *Ann Surg* 2004;239:712–9; discussion 719–21.
6. Cammà C, Schepis F, Orlando A, Albanese M, Shahied L, Trevisani F, et al. Transarterial chemoembolization for unresectable hepatocellular carcinoma: meta-analysis of randomized controlled trials. *Radiology* 2002;224:47–54.
7. Llovet JM, Bruix J. Systematic review of randomized trials for unresectable hepatocellular carcinoma: chemoembolization improves survival. *Hepatology* 2003;37:429–42.
8. Dawson LA, Ten Haken RK. Partial volume tolerance of the liver to radiation. *Semin Radiat Oncol* 2005;15:279–83.
9. Nakagawa K, Yamashita H, Shiraishi K, Nakamura N, Tago M, Igaki H, et al. Radiation therapy for portal venous invasion by hepatocellular carcinoma. *World J Gastroenterol* 2005;11:7237–41.
10. Huang CJ, Lian SL, Chen SC, Wu DK, Wei SY, Huang MY, et al. External beam radiation therapy for inoperable hepatocellular carcinoma with portal vein thrombosis. *Kaohsiung J Med Sci* 2001;17:610–4.
11. Tazawa J, Maeda M, Sakai Y, Yamane M, Ohbayashi H, Kakinuma S, et al. Radiation therapy in combination with transcatheter arterial chemoembolization for hepatocellular carcinoma with extensive portal vein involvement. *J Gastroenterol Hepatol* 2001;16:660–5.
12. Ishikura S, Ogino T, Furuse J, Satake M, Baba S, Kawashima M, et al. Radiotherapy after transcatheter arterial chemoembolization for patients with hepatocellular carcinoma and portal vein tumor thrombus. *Am J Clin Oncol* 2002;25:189–93.
13. Yamada K, Izaki K, Sugimoto K, Mayahara H, Morita Y, Yoden E, et al. Prospective trial of combined transcatheter arterial chemoembolization and three-dimensional conformal radiotherapy for portal vein tumor thrombus in patients with unresectable hepatocellular carcinoma. *Int J Radiat Oncol Biol Phys* 2003;57:113–9.
14. Kim DY, Park W, Lim DH, Lee JH, Yoo BC, Paik SW, et al. Three-dimensional conformal radiotherapy for portal vein thrombosis of hepatocellular carcinoma. *Cancer* 2005;103:2419–26.
15. Lin CS, Jen YM, Chiu SY, Hwang JM, Chao HL, Lin HY, et al. Treatment of portal vein tumor thrombosis of hepatoma patients with either stereotactic radiotherapy or three-dimensional conformal radiotherapy. *Jpn J Clin Oncol* 2006;36:212–7.
16. Zeng ZC, Fan J, Tang ZY, Zhou J, Qin LX, Wang JH, et al. A comparison of treatment combinations with and without radiotherapy for hepatocellular carcinoma with portal vein and/or inferior vena cava tumor thrombus. *Int J Radiat Oncol Biol Phys* 2005;61:432–43.
17. Llovet JM, Bustamante J, Castells A, Vilana R, Ayuso Mdel C, Sala M, et al. Natural history of untreated nonsurgical hepatocellular carcinoma: rationale for the design and evaluation of therapeutic trials. *Hepatology* 1999;29:62–7.
18. The Cancer of the Liver Italian Program (CLIP) Investigators. A new prognostic system for hepatocellular carcinoma: a retrospective study of 435 patients. *Hepatology* 1998;28:751–5.
19. Mizumoto M, Tokuuye K, Sugahara S, Hata M, Fukumitsu N, Hashimoto T, et al. Proton beam therapy for hepatocellular carcinoma with inferior vena cava tumor thrombus: report of three cases. *Jpn J Clin Oncol* 2007;37:459–62.
20. Franco D, Capussotti L, Smadja C, Bouzari H, Meakins J, Kemeny F, et al. Resection of hepatocellular carcinomas: results in 72 European patients with cirrhosis. *Gastroenterology* 1990;98:733–8.
21. Okuda K. Natural history of hepatocellular carcinoma including fibrolamellar and hepato-cholangiocarcinoma variants. *J Gastroenterol Hepatol* 2002;17:401–5.
22. Chen CH, Chang TT, Cheng KS, Su WW, Yang SS, Lin HH, et al. Do young hepatocellular carcinoma patients have worse prognosis? The paradox of age as a prognostic factor in the survival of hepatocellular carcinoma patients. *Liver Int* 2006;26:766–73.
23. Liem MS, Poon RT, Lo CM, Tso WK, Fan ST. Outcome of transarterial chemoembolization in patients with inoperable hepatocellular carcinoma eligible for radiofrequency ablation. *World J Gastroenterol* 2005;11:4465–71.
24. Wu DH, Liu L, Chen LH. Therapeutic effects and prognostic factors in three-dimensional conformal radiotherapy combined with transcatheter arterial chemoembolization for hepatocellular carcinoma. *World J Gastroenterol* 2004;10:2184–9.
25. Kayama T, Kumabe T, Tominaga T, Yoshimoto T. Prognostic value of complete response after the initial treatment for malignant astrocytoma. *Neurol Res* 1996;18:321–4.
26. Willers H, Wurschmidt F, Bunemann H, Heilmann HP. High-dose radiation therapy alone for inoperable non-small cell lung cancer—experience with prolonged overall treatment times. *Acta Oncol* 1998;37:101–5.
27. Kostakoglu L, Goldsmith SJ. PET in the assessment of therapy response in patients with carcinoma of the head and neck and of the esophagus. *J Nucl Med* 2004;45:56–68.
28. Lawrence TS, Robertson JM, Anscher MS, Jirtle RL, Ensminger WD, Fajardo LF. Hepatic toxicity resulting from cancer treatment. *Int J Radiat Oncol Biol Phys* 1995;31:1237–48.

29. Dawson LA, Normolle D, Balter JM, McGinn CJ, Lawrence TS, Ten Haken RK. Analysis of radiation-induced liver disease using the Lyman NTCP model. *Int J Radiat Oncol Biol Phys* 2002;53:810–21.
30. Cheng JC, Wu JK, Huang CM, Liu HS, Huang DY, Cheng SH, et al. Radiation-induced liver disease after three-dimensional conformal radiotherapy for patients with hepatocellular carcinoma: dosimetric analysis and implication. *Int J Radiat Oncol Biol Phys* 2002;54: 156–62.
31. Xu ZY, Liang SX, Zhu J, Zhu XD, Zhao JD, Lu HJ, et al. Prediction of radiation-induced liver disease by Lyman normal-tissue complication probability model in three-dimensional conformal radiation therapy for primary liver carcinoma. *Int J Radiat Oncol Biol Phys* 2006;65: 189–95.
32. Fowler JF. The linear–quadratic formula and progress in fractionated radiotherapy. *Br J Radiol* 1989;62:679–94.

hScrib, a human homologue of *Drosophila* neoplastic tumor suppressor, is a novel death substrate targeted by caspase during the process of apoptosis

Kenbun Sone[1], Shunsuke Nakagawa[1,*], Keiichi Nakagawa[2], Shin Takizawa[1], Yoko Matsumoto[1], Kazunori Nagasaka[1], Tetsushi Tsuruga[1], Haruko Hiraike[1], Osamu Hiraike-Wada[1], Yuichiro Miyamoto[1], Katsutoshi Oda[1], Toshiharu Yasugi[1], Koji Kugu[1], Tetsu Yano[1] and Yuji Taketani[1]

[1]*Department of Obstetrics and Gynecology, and*
[2]*Department of Radiology, Graduate School of Medicine, The University of Tokyo, 7-3-1 Hongo, Bunkyo-ku, Tokyo 113-8655, Japan*

hScrib, human homologue of *Drosophila* neoplastic tumor suppressor, was identified as a target of human papillomavirus E6 oncoprotein for the ubiquitin-mediated degradation. Here, we report that hScrib is a novel death substrate targeted by caspase. Full-length hScrib was cleaved by caspase during death ligands-induced apoptosis, which generates a p170 C-terminal fragments in Hela cells. *In vitro* cleavage assay using recombinant caspases showed that hScrib is cleaved by the executioner caspases. DNA damage-induced apoptosis caused loss of expression of full-length hScrib, which was recovered by addition of capase-3 inhibitor in HaCat cells. TUNEL positive apoptotic cells, which were identified 4 h after UV irradiation in HaCat cells, showed loss of hScrib expression at the adherens junction. Mutational analysis identified the caspase-dependent cleavage site of hScrib at the position of Asp-504. Although MDCK cells transfected with GFP-fused wild-type hScrib showed loss of E-cadherin expression and shrinkage of cytoplasm by UV irradiation, cells transfected with hScrib with Ala substitution of Asp-504 showed resistance to caspase-dependent cleavage of hScrib and intact expression of E-cadherin. These results indicate that caspase-dependent cleavage of hScrib is a critical step for detachment of cell contact during the process of apoptosis.

Introduction

Programmed cell death and morphological apoptosis is an intrinsic mechanism of self-destruction of cells (Steller 1995). Well-defined programmed cell death mechanism is crucial for successful embryogenesis and organogenesis (Jacobson *et al.* 1997). Disturbance of the apoptotic functions, which govern homeostasis of tissues, causes proliferation of overgrowing cells and leads to the tumor formation. The apoptotic surveillance mechanism usually causes fragmentation of chromosome and elimination of uncontrolled over-proliferated cells. Cancer cells are considered to develop by escaping from the cellular surveillance mechanisms governing tissue homeostasis. We previously identified hScrib as a target protein of high-risk human papillomavirus (HPV) E6 oncoprotein, which is considered to have a causal role in development of cervical cancer, for the ubiquitin-mediated degradation (Nakagawa & Huibregtse 2000). hScrib is shown to regulate cell cycle progression depending on its association with tumor suppressor protein adenomatous polyposis coli (APC) (Nagasaka *et al.* 2006; Takizawa *et al.* 2006). *Drosophila* Scribble localizes at the septate junction, which is functionally identical to the mammalian tight junction (Bilder & Perrimon 2000). hScrib localizes at the adherens junction in the epithelial MDCK cells (Nakagawa *et al.* 2004). Cysteine proteases from caspase family, which cleave their target proteins exclusively after the Asp residue, have an important function in the process of apoptosis (Brancolini *et al.* 1997; Nicholson & Thornberry 1997; Salvesen & Dixit 1997). Many proteins localized at the adherens junction are targeted by caspase for their cleavage. For instance, β-catenin (Brancolini *et al.* 1997), E-cadherin, plakoglobin, focal adhesion kinase (Levkau *et al.* 1998) and human Discs large (hDlg) (Gregorc *et al.*

Communicated by: Tadashi Yamamoto
**Correspondence:* Email: nakagawas-tky@umin.ac.jp

DOI: 10.1111/j.1365-2443.2008.01204.x

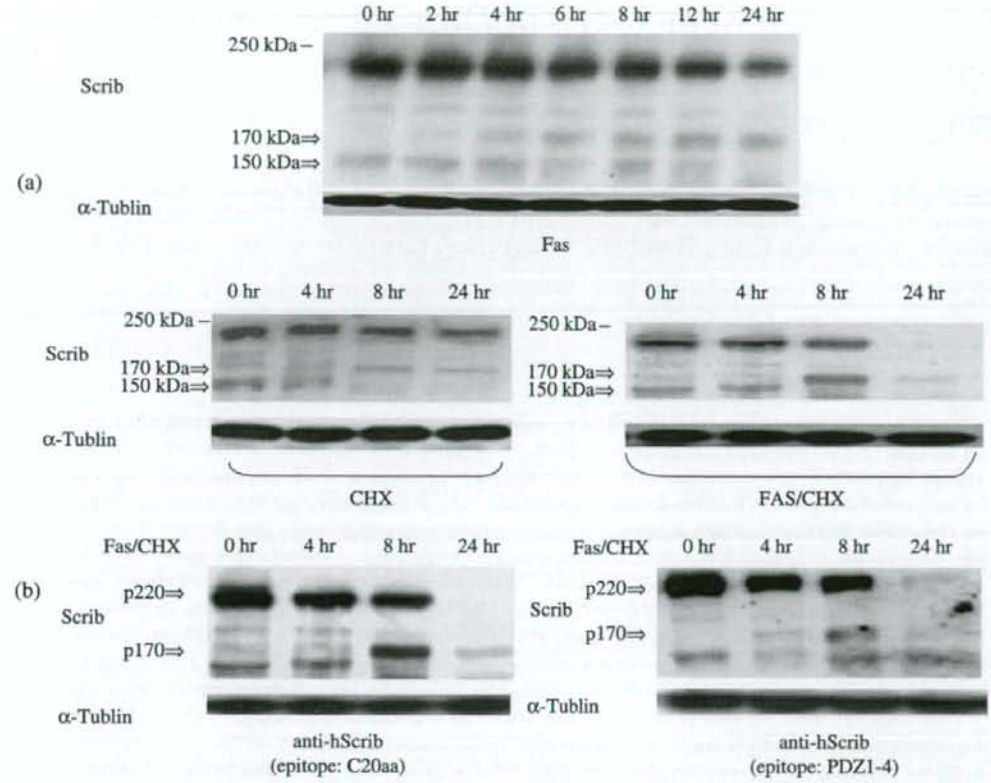

Figure 1 Cleavage of hScrib in Hela cells during Fas ligand-induced apoptosis. (a) HeLa cells were treated with Fas, CHX alone or Fas–CHX. Samples were taken at the times indicated. Western blotting as described in the Material and methods section monitored the amount of hScrib. The expression α-Tublin was shown as the internal control for each lane. (b) The cleavage of hScrib during apoptosis induced by Fas–CHX was analyzed by Western blotting with two antibodies raised against two different hScrib antigens. Note that p220 and p170 hScrib were detected by both of two antibodies. (Correction added after online publication 30 May 2008: This is the corrected version of Figure 1.)

2005) are cleaved by caspase during the process of apoptosis. Here, we identified that hScrib is targeted by caspase for cleavage during the process of apoptosis induced by death ligands and DNA damages.

Results

hScrib is cleaved during the process of apoptosis induced by death ligands and DNA damage

hScrib was shown to be cleaved and generate p170 hScrib during the process of apoptosis induced by death ligand, Fas (Fig. 1a). The band of full-length hScrib p220 and that of p170 generated by induction of apoptosis with Fas ligand and Cycloheximide (CHX) were identified by the two anti-hScrib antibodies raised against different epitopes (Fig. 1b). These data indicate that the full-length hScrib (p220) was cleaved during apoptosis and p170 hScrib was the cleaved product of full-length hScrib. There is one additional band in the lane of 0 h (p150, Figs 1, 2), which also disappeared by Fas–CHX or TNF–CHX treatment. This endogenous p150 was also identified by immunoblotting analysis with two anti-hScrib antibodies (Fig. 1b). The origin of p150 hScrib is currently unknown. The addition of CHX augmented cleavage of hScrib by the induction of apoptosis induced by Fas ligand (Fig. 1a). The hScrib p220 was completely disappeared 24 h after Fas–CHX or TNF–CHX treatment (Figs 1, 2). These data indicate that apoptosis activation by Fas ligand or TNF requires coordinate inhibition of

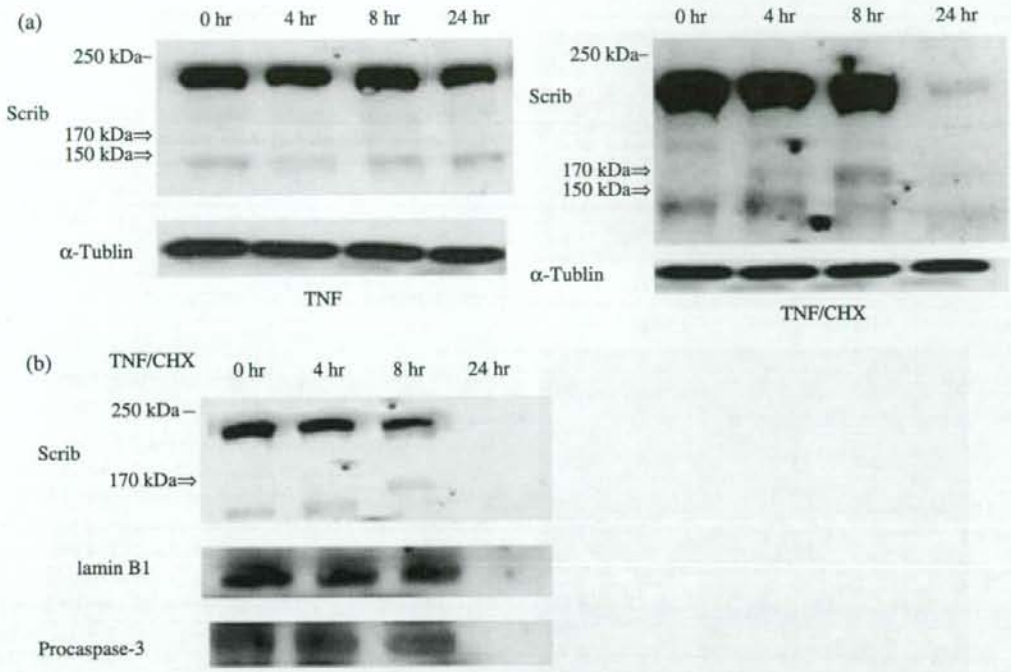

Figure 2 Cleavage of hScrib in Hela cells during TNF-induced apoptosis. (a) HeLa cells were treated with TNF alone or TNF–CHX. Samples were taken at the times indicated and the amount of hScrib was monitored by Western blotting. (b) The efficiency of cleavage of hScrib by the TNF–CHX treatment was compared with that of Lamin B1 or procaspase-3. The efficiency of cleavage of hScrib during apoptosis induced by UV irradiation was equivalent to that of Lamin B1 or procaspase-3. (Correction added after online publication 30 May 2008: This is the corrected version of Figure 2.)

survival signal that inhibit generation of prosurvival factors mediated by NF-κB (Perez & White 2000; Kucharczak *et al.* 2003). The cleavage of hScrib and generation of p170 hScrib were not observed by only TNF ligand, but by the combination of TNF ligand with CHX (Fig. 2a). We compared the efficiency of cleavage of hScrib by the TNF–CHX treatment with that of Lamin B1 or procaspase-3, which are reported to be the early targets for cleavage by caspase during apoptosis (Samejima *et al.* 1999). The efficiency of cleavage of hScrib during apoptosis induced by UV irradiation was equivalent to that of Lamin B1 or procaspase-3 (Fig. 2b).

hScrib localizes at the adherens junction in normal cells as previously reported (Fig. 3a) (Nakagawa *et al.* 2004). DNA damage by UV irradiation caused loss of expression of hScrib at the adherens junction in the apoptotic cells showing condensed (Fig. 3, arrow) or fragmented (Fig. 3, arrow head) nucleus showed by the Hoechst staining.

Loss of expression of hScrib is an early event during apoptosis-induced DNA damage

UV irradiation induced progressive decrease of hScrib expression at the cellular membrane along with time after UV irradiation (Fig. 4). Loss of hScrib expression was identified in the TUNEL positive cells after 4 h of UV irradiation (Fig. 4 UV4 h, arrow indicates TUNEL positive cells, which lost membrane bound expression of hScrib). These data suggest the possibility that hScrib in involved in the cellular detachment at the adherens junction in the early stage of apoptosis. The involvement of hDlg in elimination of apoptotic cell from cellular contact with normal cells, has been reported (Gregorc *et al.* 2005). We analyzed loss of expression of these tumor suppressors in Caco-2 cells, as these tumor suppressors are human homologues of *Drosophila* neoplastic tumor suppressors, in which mutation causes loss of tissue architecture and overgrowth of epithelial cells (Bilder &

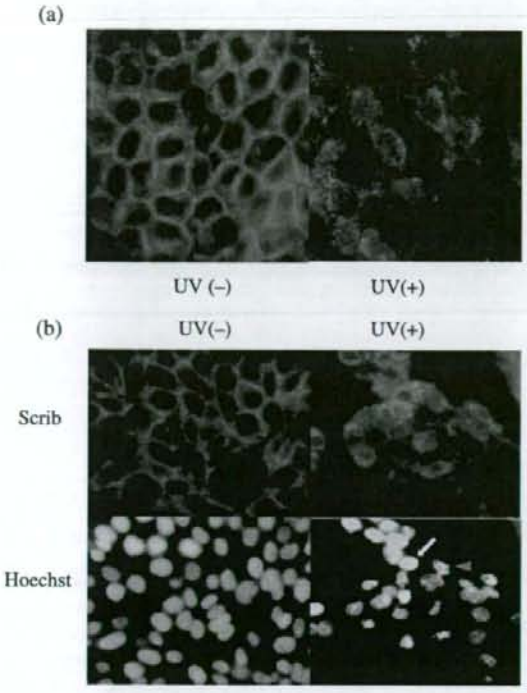

Figure 3 Loss of hScrib expression by the apoptosis induced by UV irradiation in HaCaT cells. (a) Apoptosis was induced with UV irradiation as described in the Materials and methods. Immunofluorescence images with anti-hScrib antibody were taken under the confocal microscopy before and after 6 h of UV irradiation. (b) Loss of hScrib expression at the cellular membrane was observed in the apoptotic cells showing condensed (arrow) or fragmented (arrow head) nucleus showed by the Hoechst staining.

Perrimon 2000). As shown in Fig. 5, the expressed level of hDlg in Caco-2 cells 8 h after UV irradiation was almost equivalent to that of untreated cells (Fig. 5a). In contrast, expression of hScrib was almost diminished in cells after 8 h of UV irradiation (Fig. 5a). Immunofluorescence analysis showed that the membrane-bound expression of hScrib was not observed, and it showed that dot-like expression, whereas hDlg still showed the membrane-bound expression in cells after 6 h of UV irradiation (Fig. 5b). At 12 h after irradiation of UV, expression of hScrib was not observed, but hDlg showed still faint but membrane-associated expression (Fig. 5b). These results indicate that hSrib is targeted by proteolysis earlier than the hDlg in apoptotic cells induced by UV irradiation.

hScrib is cleaved by the executioner caspases *in vitro*

Based on data described above, we investigated the possibility that hScrib is targeted for cleavage by caspase. *In vitro* translated hScrib was incubated with recombinant caspase-3, caspase-6, caspase-7 or caspase-8. hScrib was cleaved *in vitro* by the executioner caspases, caspase-3, caspase-6 and caspase-7 (Fig. 6a). The *in vitro* cleavage of hScrib by caspase-3 was completely repressed by the caspase-3 inhibitor (Fig. 6b). These data indicate that hScrib is a novel death substrate targeted by the executioner caspases.

hScrib is targeted by executioner caspase for proteolysis during the process of apoptosis

Next, we investigated the possibility that hScrib is targeted for cleavage by caspase *in vivo* during apoptosis. Apoptosis induced by UV irradiation caused cleavage of hScrib as mentioned above (Fig. 7). Loss of expression of hScrib as a result of cleavage by caspase activated with UV irradiation was recovered by addition of the caspase-3 inhibitor in the medium (Fig. 7). The caspase-6 inhibitor also showed the repressive effect on the cleavage of hScrib during apoptosis, but its inhibitory effect was weaker than that of caspase-3 inhibitor (Fig. 7). These data indicate that hScrib is targeted for cleavage during the process of apoptosis mainly by caspase-3.

504 Asp of hScrib is critical for caspase-dependent cleavage

Asp-X-X-Asp is reported to be conserved motif for caspase-dependent cleavage (Nicholson & Thornberry 1997; Talanian *et al.* 1997). There are two putative caspase-dependent cleave sites with amino acids Asp-X-X-Asp at 1068 Asp-X-X-1071 Asp and at 1131 Asp-X-X-1134 in amino acids sequence of hScrib. Alanine substitution of these Asp amino acids did not allow hScrib to resist to caspase-dependent cleavage (data not shown). hScrib consists of 16 canonical Leucine rich repeats (LRRs), LAP specific domain-a (LAPSD-a), LAPSD-b and four PDZ domains. We investigated which domains of hScrib are susceptible for cleavage by caspase *in vitro* by using several hScrib C-terminal deletion mutants. Human Scrib mutants, LRR–PDZ3, LRR–PDZ2 and LRR–PDZ1 were cleaved by recombinant caspase-3, whereas LRR–LAPSD and LRR were not susceptible for cleavage. These data indicate that hScrib is cleaved by caspase-3 at the C-terminal region of LAPSD (Fig. 8a). Mutational analysis found that Ala substitution of Asp 504 allows hScrib to resist to caspase-3 dependent cleavage (Fig. 8b).

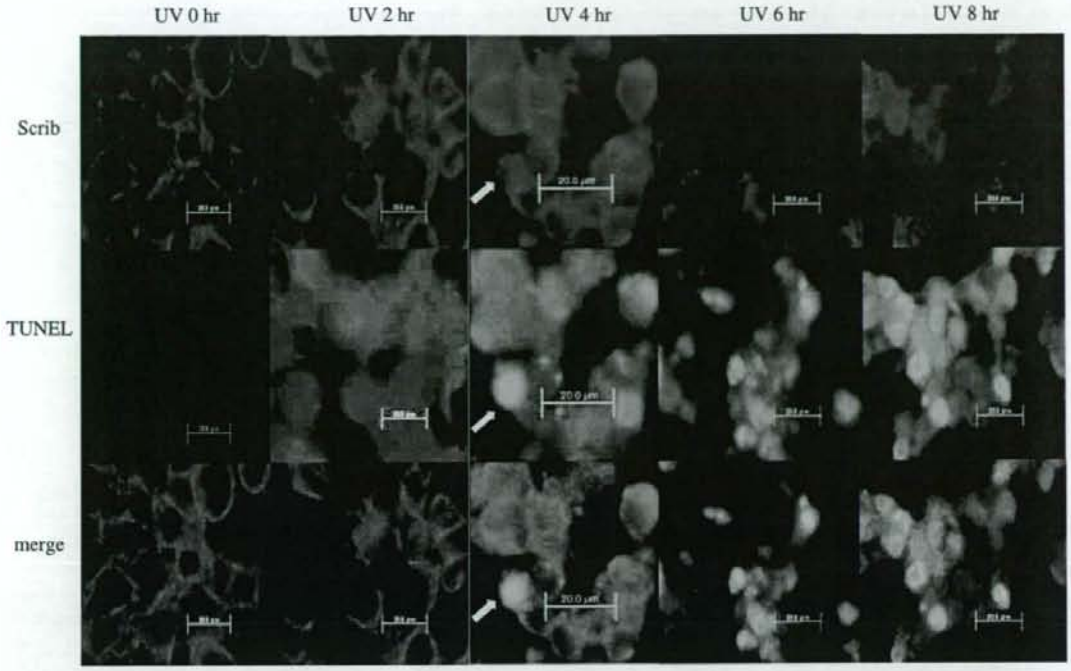

Figure 4 Loss of hScrib expression is an early event during apoptotic process. Cells irradiated with UV were analyzed by immunofluorescence staining with anti-hScrib antibody and TUNEL at the indicated time after UV irradiation. Note that hScrib expression was lost in the TUNEL positive cell (UV 4 h). The arrow indicates that loss of hScrib expression is observed in the TUNEL positive cells after 4 h of UV irradiation.

Alanine substitution of Asp 526 resided at the C-terminus of the LAPD of hScrib did not render hScrib resistant to caspase-3 dependent cleavage (Fig. 8b).

hScrib with Ala substitution of Asp 504 is resistant to caspase-dependent cleavage during the process of apoptosis induced by UV irradiation

GFP-tagged wild-type hScrib transfected MDCK cells showed loss of E-cadherin and hScrib expression at the membrane, fragmentation of nucleus and shrinkage of cytoplasm by apoptosis induction with UV irradiation (Fig. 9a,b). In contrast, GFP-tagged Asp504Ala hScrib mutant transfected MDCK cells showed the intact expression of transfected hScrib and E-cadherin, despite of fragmentation of nucleus showed by the Hoechst staining (Fig. 9c,d). Immunoblotting analysis confirmed that over-expressed GFP–hScrib D504A mutant is resistant to caspase-dependent cleavage activated by apoptosis induction with UV irradiation (Fig. 10a). To quantify the effect of WT and Asp504Ala hScrib mutant on apoptosis induction and cellular detachment, 300 MDCK cells transfected with control vector, GFP–WT hScrib vector, or GFP–hScrib D504A mutant vector were analyzed for apoptosis signals and cellular detachment by Hoechst staining and immunofluorescence analysis of E-cadherin, respectively (Fig. 10b). UV irradiation induced apoptosis and cellular detachment approximately in 80% MDCK cells transfected with control vector or GFP–WT hScrib vector. Although apoptosis was observed over 80% of cells transfected with GFP–hScrib D504A mutant vector, cellular detachment was only observed in 9% of those cells. These data indicate that caspase-dependent cleavage of hScrib has a crucial role in cellular detachment during progression of apoptosis.

Effect of HPV E6 expression on the caspase-dependent cleavage of hScrib during apoptosis

We investigated whether E6 expression have an effect on caspase-dependent cleavage of hScrib. As shown in Fig. 11, hScrib expression level in cells transfected with E6